Available online at www.sciencedirect.com
SCIENCE DIRECT®
Journal of Solid State Chemistry 177 (2004) 1520–1528
JOURNAL OF SOLID STATE CHEMISTRY
http://elsevier.com/locate/jssc

Multiple-step preparation and physicochemical characterization of crystalline α-germanium hydrogenphosphate

Ricardo Romano,[a,*] Ana I. Ruiz,[b] and Oswaldo L. Alves[a]

[a] *Laboratório de Química do Estado Sólido, Instituto de Química, Universidad Estudual de Campinas, UNICAMP, CP 6154, 13084-971 Campinas, SP, Brazil*

[b] *Dpto. Química Inorgánica I, Facultad de CC. Químicas, Universidad Complutense de Madrid, 28040 Madrid, Spain*

Received 3 July 2003; received in revised form 27 November 2003; accepted 8 December 2003

Abstract

The reaction between germanium oxide and phosphoric acid has previously been described and led to impure germanium hydrogenphosphate samples with low crystallinity. A new multiple-step route involving the same reaction under refluxing and soft hydrothermal conditions is described for the preparation of pure and crystalline α-GeP. The physicochemical characterization of the samples allows accompaniment of the reaction evolution as well as determining short- and long-range structural organization. The phase purity of the α-GeP sample was confirmed by applying Rietveld's profile analysis, which also determined the cell parameters of its crystals.

Keywords: A. Layered compounds; B. Chemical synthesis; C. Infrared spectroscopy; C. Nuclear magnetic resonance (NMR); C. Thermogravimetric analysis (TGA); C. X-ray diffraction

1. Introduction

Acid phosphates of tetravalent metals (APTM) have been the object of increasing interest over the last several decades owing to such properties as high cation-exchange capacity and high resistance towards elevated temperature and ionizing radiation. From 1956 onward, such features turned attention to possible applications of these materials, in their amorphous forms, in currently established nuclear technology. The first preparation of a crystalline APTM in 1964, as well as the first structural elucidation in 1969, were carried out by Clearfield et al. [1,2]. Several insoluble APTMs were obtained as crystalline compounds since, and these materials were found to be more stable than the amorphous ones [3]. These features, in addition to its layered structure, have brought a renewed interest for APTMs as host matrices for the preparation of nanocomposite solids via intercalation of organic molecules [4,5] and polymers [5–12].

This paper describes a new route for the preparation of pure and highly crystalline α-germanium hydrogenphosphate (α-GeP), the least known and studied APTM, by reacting germanium oxide and phosphoric acid in a multiple step process. Previous studies on this reaction were performed by Everest [13], Lelong [14], Avduevskaya and Tananaev [15,16], and Winkler and Thilo [17]. The first author cited obtained an impure crystalline precipitate corresponding to the anhydrous phase $Ge(HPO_4)_2$. Lelong [14] reported X-ray diffraction (XRD) patterns and thermogravimetric analyses for hydrated germanium acid phosphate, $Ge(HPO_4)_2 \cdot H_2O$, which, according to La Ginestra et al. [18], suggest that the material is a not pure compound. Avduevskaya and Tananaev [15,16] have also reported XRD patterns for hydrated germanium acid phosphate as well as for its anhydrous phase and these results also pointed out that the solids were probably not pure phases [18]. Winkler and Thilo [17] synthesized a series of APTM including germanium, silicon, lead, zirconium, titanium, and tin analogues. Despite the poor degree of crystallinity, they were able to characterize the isostructurality of these acid phosphates.

La Ginestra et al. [18] described the conditions which they have considered as being optimum for obtaining germanium acid phosphate as a pure, crystalline compound, by refluxing germanium tetrachloride in

*Corresponding author. Fax: +55-19-37883023.
E-mail addresses: rromano@iqm.unicamp.br (R. Romano), oalves@iqm.unicamp.br (O.L. Alves).
URL: http://lqes.iqm.unicamp.br.

0022-4596/$ - see front matter © 2003 Elsevier Inc. All rights reserved.
doi:10.1016/j.jssc.2003.12.002

phosphoric acid. Nevertheless, their conclusions were based only on thermal analysis and XRD pattern observations, techniques that do not evaluate the extension of order on the short-range scale. However, their results characterized once more the isostructurality of germanium acid phosphate and the most studied compounds of its class: α-zirconium and α-titanium hydrogenphosphates, whose crystalline structures were already elucidated and known as the α-layered phase [19,20].

Generally, preparations of APTM performed by refluxing the amorphous gels in phosphoric acid give rise to solids showing poor long-range ordering even after extended periods of reaction. To overcome this problem, attempts to prepare APTM with improved crystallinity in a shorter time have used treatments under hydrothermal conditions at 200–300°C. This approach has been successfully employed for obtaining highly crystalline α-zirconium, α-titanium, and α-tin hydrogenphosphates [21] in addition to cerium (IV) acid phosphate [22]. Previous studies have not achieved similar results for α-GeP. Its reduced chemical stability, common to germanium salts, led to the formation of the hydrolysis product, instead of highly crystalline α-GeP, after only a few hours of treatment at 180°C [21].

In addition to preparation methods of α-GeP described above, studies concerning its thermal behavior [16,18], preparation of solid solutions with different APTMs [23,24], and catalytic [21] and ion-exchange capacities [17] have also been reported. Its physicochemical characterization is very restricted and, to our knowledge, no studies exploring the potentialities of α-GeP as a host matrix in intercalation processes has yet been reported.

These various aspects provided the impetus for the research reported here, in which we evaluate the possibilities of obtaining α-GeP with improved crystallinity by the refluxing method followed by a soft hydrothermal treatment. Since in the past the reaction between germanium oxide and phosphoric acid led to impure, poorly crystalline solids, the evolution of the reaction and also structural ordering of the product were monitored by a set of physicochemical techniques including X-ray powder diffraction, FT infrared and ^{31}P magic angle spinning nuclear magnetic resonance spectroscopies, scanning electron microscopy, chemical and thermal analyses.

2. Experimental

2.1. Materials

All chemicals were used without further purification. Germanium (IV) oxide (99.9999%) and phosphoric acid were obtained from Aldrich and Merck, respectively.

Table 1
Steps for preparation of α-GeP samples

Sample	Preparation steps
α-GeP-14	14 h of refluxing
α-GeP-25	25 h of refluxing
α-GeP-100	25 + 100 h of refluxing
α-GeP-720	25 + 100 h of refluxing + 720 h of hydrothermal treatment

2.2. Preparation of α-GeP samples

The previous studies on the reaction between germanium oxide and phosphoric acid, commented above [13–17], were taken as a starting point for the precipitation of α-GeP. To an aqueous phosphoric acid solution (70 cm^3, 85%) preheated to 90°C, 6.0 g of germanium oxide dispersed in 20 cm^3 of distilled water were added drop wise. Samples of the precipitate were extracted after 14 and 25 h of refluxing. The solids were centrifuged, thoroughly washed with pure ethanol, and dried under dynamic vacuum.

A 1.25 g sample of the 25 h-refluxed compound was submitted to a subsequent reflux process in phosphoric acid solution (40 cm^3, 12 mol dm^{-3}) for 100 h. After this time, a 0.5 g of the recovered solid was introduced into a glass tube containing a phosphoric acid solution (6 cm^3, 12 mol dm^{-3}). The sealed tube was heated at 100°C for 720 h and at the end of this period the solid was recovered as described above. Table 1 identifies the samples obtained and summarizes the steps for their preparation.

2.3. Analytical procedures

The P:Ge molar ratio of the α-GeP samples was determined by X-ray fluorescence (XRF) on a Shimadzu EDX-700 apparatus using GeO_2 and KH_2PO_4 as Ge and P standards, respectively. XRD measurements were performed on a Carl Zeiss URD-6 powder diffractometer using Cu$K\alpha$ radiation. Rietveld method and the Fullprof program [25] were applied to the analysis of a XRD pattern of α-Ge-720 sample which was registered by means of a Shimadzu XRD-6000 powder diffractometer operating whit Cu$K\alpha$ radiation, step size of 0.04°, and counting time of 20 s for each step. FTIR spectra were obtained on a Bomem MB-series spectrometer. Samples were prepared as "Nujol" and "Fluorolube" mulls. The ^{31}P nuclear magnetic signal spectra with magic angle spinning (^{31}P MAS NMR) were obtained at 202.35 MHz on a Varian Inova 500 spectrometer at 4.0 kHz. Chemical shifts were determined with respect to an external standard of H_3PO_4. Scanning electron microscopy (SEM) was carried out on a MEV JEOL JSM T-300 Microscope. TGA measurements were performed under air on a TA Instruments

500 TGA 2050 using a heating rate of $10^{\circ}C\,min^{-1}$ and platinum crucibles.

3. Results and discussion

3.1. Powder X-ray diffraction

Comparison of the XRD data obtained for GeO_2 and for α-GeP samples is presented in Fig. 1. The XRD patterns are arranged in order to allow a visualization of structural changes after each preparation step. The GeO_2 XRD pattern shows a main reflection at 26.0° (2θ), $d = 3.43$ Å, assigned to (101) atomic planes [26]. One can notice that the α-GeP-14 XRD pattern shows a profile very close to that of oxide, implying that the germanium precursor was not fully converted to the product after 14 h. However, the appearance of a new peak at 11.4° (2θ), related to an interlayer distance of 7.76 Å, characterizes the formation of the product phase (α-GeP) in the solid [16,18].

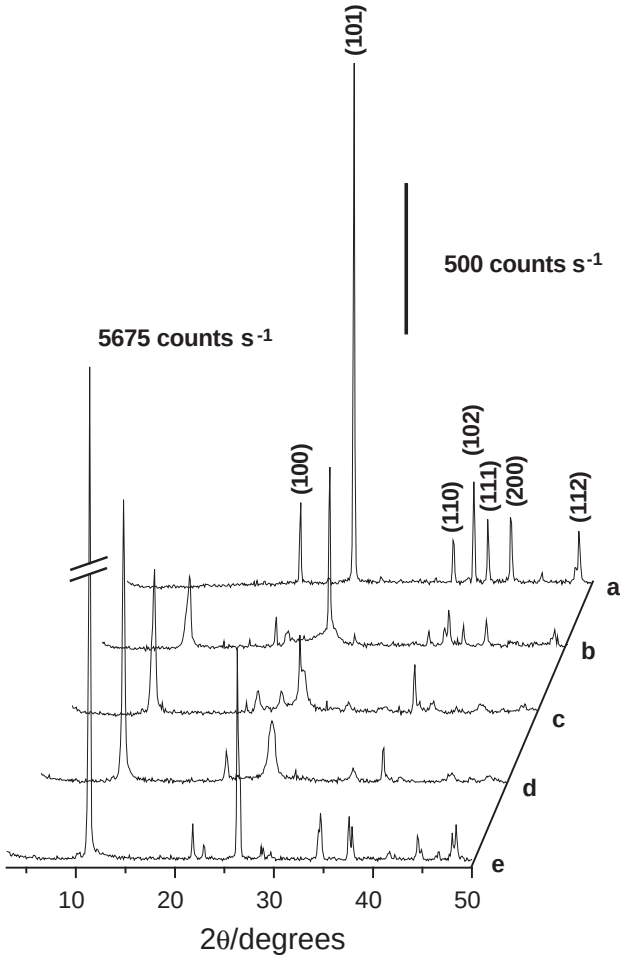

Fig. 1. Comparative graph showing the powder XRD patterns of: (a) GeO_2; (b) α-GeP-14; (c) α-GeP-25; (d) α-GeP-100; (e) α-GeP-720.

Even after 25 h of reflux, the solid still shows the oxide reflection at 26.0° (2θ). Nevertheless, its lower intensity indicates a gradual conversion of the oxide to the layered product, also characterized by an intensification of the peak at 11.4° (2θ) as well as by the detection of new reflections associated with α-GeP [16,18]. One of them, centered in 26.3° (2θ), $d = 3.39$ Å, emerged in a position very close to the main oxide reflection and covered it in the next XRD pattern (Fig. 1c), where oxide reflections were no longer observed, suggesting the absence of crystalline GeO_2 after the 100 h refluxing step. Therefore, the appreciable intensification observed for the peaks of the α-GeP-720 sample, especially for that situated around 11.4° (2θ), attributed to lamellae organization, indicates a time dependent structural ordering. This factor, together with the vanishing of the oxide reflections, suggests the obtainment of a pure and crystalline α-GeP sample after the soft hydrothermal treatment step, contrary to previous attempts, which employed more drastic hydrothermal conditions and have failed [21].

3.2. Rietveld refinement

In order to confirm the phase purity of the solid obtained after the hydrothermal treatment, a Rietveld's profile analysis method was applied to refine its X-ray powder diffraction pattern. All Bragg peaks between 5 and 60° (2θ) were indexed in a monoclinic cell with space group $P21/c$, with cell dimensions: $a = 8.230(3)$ Å; $b = 4.784(1)$ Å, $c = 16.502(5)$ Å and $\beta = 110.2(4)^{\circ}$. The unit cell volume of 609.7 $Å^3$ with four formula units per unit cell gives a density of $3.08\,g\,cm^{-3}$. The observed, calculated and difference profiles are shown in Fig. 2, which evidences a good agreement between observed and calculated patterns. Atomic coordinates obtained are given in Table 2.

The crystals of the α-GeP-720 sample show, in fact, the α-layered structure, exhibiting an interlayer distance of 7.76 Å. Each layer is formed by an intermediate Ge atom plane, in which each Ge atom is surrounded by six oxygen atoms in octahedral coordination. Moreover, metal atoms are bridged to phosphate groups located above and below the Ge atom planes, being more regular the phosphate tetrahedral of P2 than the other phosphate group (P1). The structure is shown in Fig. 3.

3.3. Elemental analysis

The P:Ge molar ratio obtained for α-GeP samples by XRF (Table 3) clearly indicates a higher relative content of germanium in the sample α-GeP-14. This result agrees with the detection of the unreacted GeO_2 characterized by the XRD powder technique.

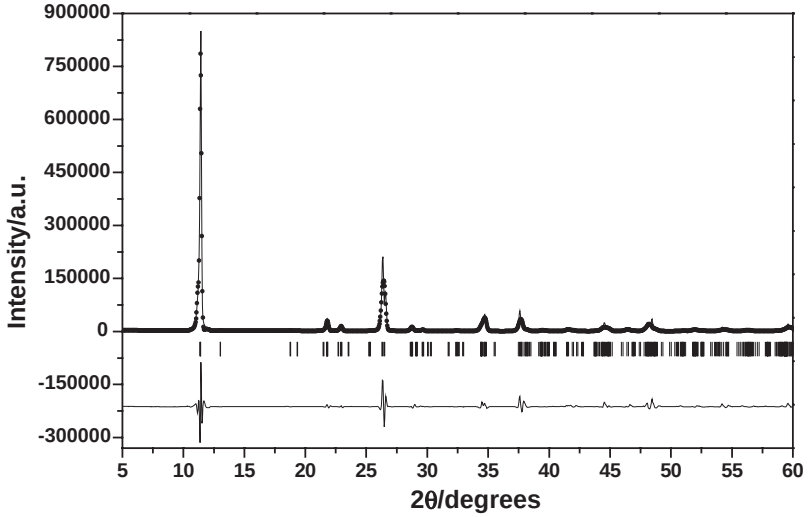

Fig. 2. Calculated (line) and observed (dots) XRD patterns and difference spectrum for α-Ge-720 ($R_p = 19.7\%$; $R_{wp} = 25.9\%$ and $R_B = 6.93\%$).

Table 2
Atomic coordinates obtained for α-GeP by Rietveld refinement

Atom	*x*	*y*	*z*
Ge	0.732(3)	0.239(1)	0.504(2)
P1	−0.022(1)	0.660(5)	0.595(5)
P2	0.479(3)	0.236(2)	0.099(3)
O1	0.136(2)	0.930(1)	0.594(2)
O2	0.912(4)	0.307(2)	0.544(2)
O3	0.836(2)	0.923(2)	0.575(5)
O4	0.163(7)	0.706(1)	0.714(3)
O5	0.318(5)	0.066(5)	0.065(3)
O6	0.403(6)	0.533(5)	0.071(5)
O7	0.613(1)	0.260(1)	0.204(4)
O8	0.356(1)	0.850(1)	0.906(5)
O9	0.268(3)	0.272(1)	0.260(8)

3.4. Thermogravimetric analysis

From the thermogravimetric (t.g.) curves of the α-GeP samples (Fig. 4) one can observe a pronounced discrepancy between the total percentage weight loss value obtained for α-GeP-14 and for the rest of samples. While the former lost around 6.4% of its initial mass before 1000°C, all other α-GeP sample lost at least 12% in the same temperature range. This once more indicates the presence of a considerable amount of GeO_2 in the solid refluxed for 14 h, agreeing with the conclusions obtained from XRD powder and XRF.

Also in agreement with XRD powder results, the t.g. curves reveal a structural ordering of the material as the samples are submitted to the consecutive treatment steps. This conclusion is evident by analyzing the first thermal event, observed between 200°C and 350°C, attributed to the loss of interlayer water molecules of α-GeP, leading to the anhydrous phase $Ge(HPO_4)_2$ [18]. One can notice this event assumes a narrow temperature range for the last samples prepared, suggesting a progressive organization of water molecules in the solid, which reflects in a progressively more ordered hydrogen bond system inside the interlayer region. Besides the narrowing of the temperature range of dehydration, this event also starts at higher temperatures for samples whose preparation involves more steps, suggesting that the organization of water molecules in the solid acts as a stabilization factor for the phase.

The following thermal event, between 400°C and 600°C, is related to the condensation of the anhydrous phase with elimination of structural water molecules, giving germanium pyrophosphate, GeP_2O_7 [18]. According to thermal studies described for α-ZrP and α-TiP [27], as well as for the α-GeP sample obtained by La Ginestra et al. [18], this event occurs in two steps, exactly as observed in the t.g. curve of the more crystalline sample, α-GeP-720.

Since we have determined the phase purity α-GeP-720 samples, and, taking into account that these samples showed mass losses nearing 6.4% at each thermal event, which could be attributed to the elimination of 1.0 mol of hydration water and 1.0 mol of structural water molecules, respectively, the chemical formulae of these samples is $Ge(HPO_4)_2 \cdot H_2O$.

3.5. ^{31}P MAS NMR spectroscopy

Earlier reports on structural elucidation [2,20] and neutron diffraction studies [28] of α-ZrP revealed the presence of two crystallographically inequivalent phosphorus sites in the α-layered structure. However, ^{31}P MAS NMR studies performed on α-ZrP [29,30] and α-TiP [31] showed only one isotropic chemical shift (ICS) for these solids. According to Clayden [29], the

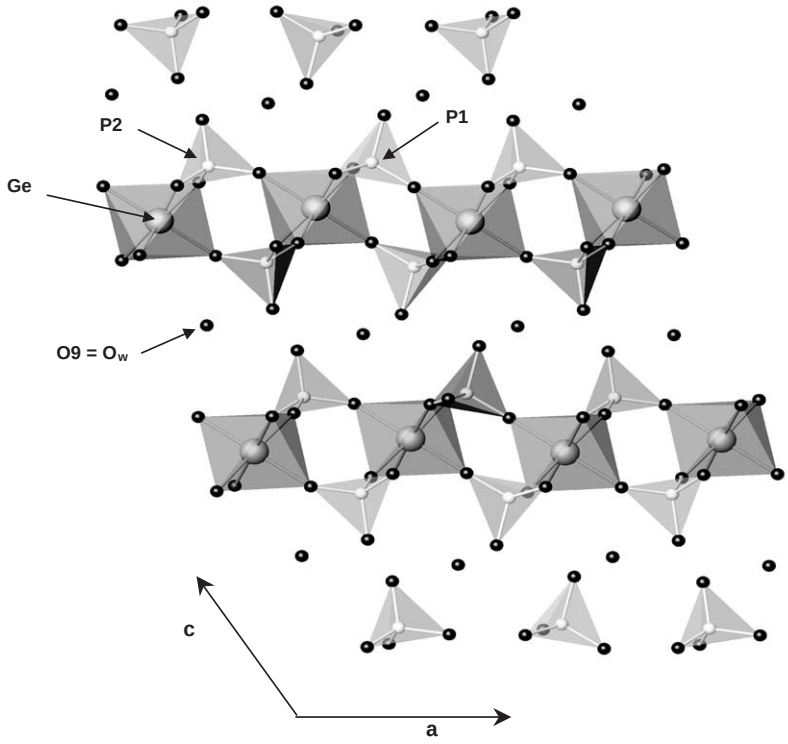

Fig. 3. Schematic view of α-layered structure obtained from the refinement of α-GeP-720 sample.

Table 3
P:Ge molar ratio obtained for α-GeP samples

Sample	P:Ge molar ratio
α-GeP-14	1.3
α-GeP-25	2.0
α-GeP-100	2.0
α-GeP-720	2.0

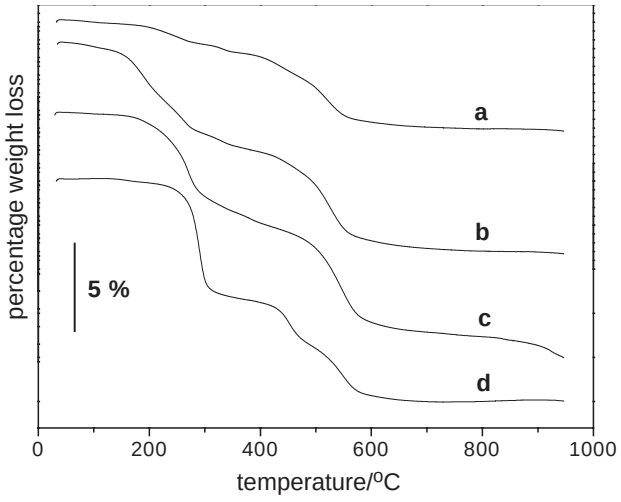

Fig. 4. t.g. Curves of the samples: (a) α-GeP-14; (b) α-GeP-25; (c) α-GeP-100; (d) α-GeP-720.

signals were not distinguished because the local electronic environment about each distinct phosphorus nucleus does not diverge sufficiently. Maclachlan and Morgan [30] presented another point of view, evaluating the effects of hydrogen bonds on the observed ICS values.

As pictured in Fig. 5, the α-layered structure contains two inequivalent sites differing slightly in their dimensions. The smaller sites allow the formation of stronger hydrogen bonds than the larger ones, being occupied preferentially. The water is hydrogen bonded to three different phosphate groups on the same layer. The pattern in the arrangement of larger and smaller sites, and the exclusive occupation of the smaller ones by water molecules in the case of a mono-hydrated salt, lead to the presence of phosphate groups interacting differently with interlayer water. One of them is observed to interact through a single hydrogen bond as donor, while the other one interacts with two different water molecules, as donor and acceptor, respectively [30].

Under circumstances in which hydrogenphosphate groups act as donors in hydrogen bonds, considering as donor the species which takes part in the bond through its acidic hydrogen atom, a downfield ^{31}P chemical shift is expected, owing to a deshielding of the phosphorus nuclei. Otherwise, acting as acceptor groups, an upfield shift is expected, since the hydrogen bonded oxygen

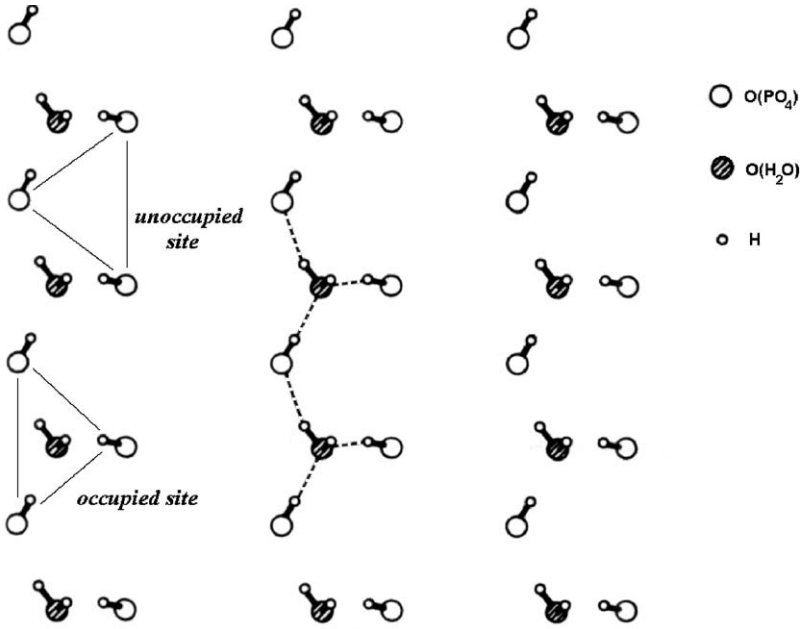

Fig. 5. Hydrogen bond system in an α-layered structure (from Ref. [29]).

atom enables a greater shielding of the phosphorus nuclei.

Maclachlan and Morgan [30] also observed that the effect resulting from interlayer water interactions on the ICS is the decrease of shielding of the phosphorus nuclei, since dehydration led to a downfield shift of +3 ppm. According to these authors, the presence of a single ICS in the α-ZrP spectrum comes from a cancellation of donor and acceptor effects. As mentioned above, one of the phosphate groups is hydrogen bonded to two water molecules. Structural determination of α-ZrP revealed that the hydrogen bond in which this group shows a donor character has a slightly smaller inter-atomic distance, being stronger than the hydrogen bond formed by the crystallographically distinct phosphate group, leading to a somewhat higher shielding effect for the latter group. However, the excess in shielding effect produced by the stronger hydrogen bond over the first group is counteracted by the deshielding effect produced by the weak acceptor hydrogen bond. Thus, both signals show very close ICS for α-ZrP, preventing their resolution.

Differently from what was observed for α-ZrP, the ^{31}P MAS NMR spectra (Fig. 6) obtained for α-GeP samples studied here presents two ICS, at −22.1 and −22.7 ppm. Their proximity to the ICS described for α-ZrP and α-TiP characterizes the presence of hydrogenphosphate groups in the α-GeP samples, since the substitution of a metallic atom coordinated to the phosphate group by a hydrogen atom leads to an ICS variation near +10 ppm [32]. In addition, the narrow discrepancy between these ICS values (0.6 ppm) suggests the presence of magnetically inequivalent phosphorus atoms in chemically identical phosphate groups, which are, thus, crystallographically different sites. This result corroborates the literature, since, to our knowledge, it shows for the first time the real presence of inequivalent phosphate groups in an α-layered hydrogenphosphate by means of a spectroscopic technique.

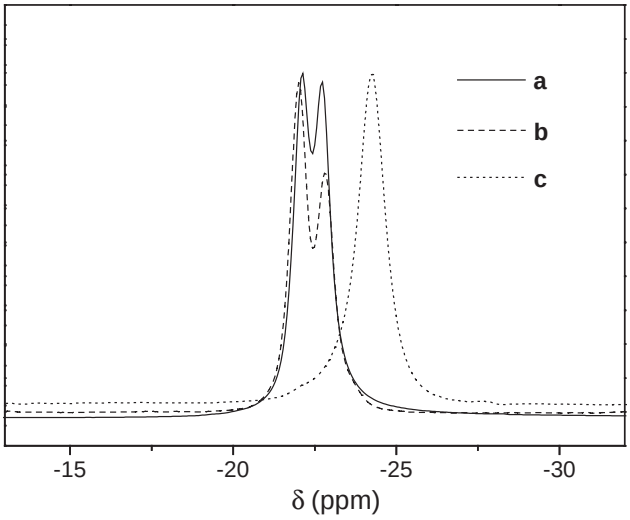

Fig. 6. Solid-state ^{31}P MAS NMR spectra for the samples: (a) α-GeP-720; (b) α-GeP-100; (c) $Ge(HPO_4)_2$.

Fig. 6 also presents the ^{31}P MAS NMR spectrum obtained for the anhydrous α-GeP. The observation of a single signal indicates that the resolution of the signals in the α-GeP spectra is really a consequence of the different interactions maintained by phosphate groups with interlayer water.

From comparison of the ICS between anhydrous and mono-hydrated α-GeP, it appears that the overall effect of hydrogen bonds on both inequivalent phosphate groups is the downfield shift. We believe that the probable reason for the resolution of the two signals in α-GeP spectra, not observed for α-ZrP and α-TiP, is a more efficient shielding effect over the phosphorus nuclei by the acceptor hydrogen bond.

An estimate on the effect of hydrogen bonds on the ICS of phosphate groups can be made by attributing the signal centered at −22.1 ppm to the groups having a single hydrogen bond with donor character, and the signal found at −22.7 ppm to the groups interacting through two hydrogen bonds. This approach reveals that, for α-GeP, the phosphate groups involved in hydrogen bonds assuming donor and acceptor character have their ICS downfielded by 2.2 ppm, and upfielded by 0.6 ppm, respectively.

This attribution allows us to interpret the pronounced differences in the intensities presented by the signals in the α-GeP-100 spectrum, which are strongly reduced for α-GeP-720. Since in an ideal α-layered structured material the crystallographically distinct phosphates should appear in the same quantity, the larger intensity of the signal attributed to the phosphate group which maintains a single donor hydrogen bond in the α-GeP-100 spectrum allows us to make some conclusions about the crystallization process of the solid. This observation points out that the water molecules initially form the stronger hydrogen bonds, where the phosphate groups have donor character. Therefore, the weaker hydrogen bonds, where phosphates have acceptor character, are formed when the water sites become more organized, a situation acquired during the crystallization process. For the α-GeP-720 sample, the signal intensities differ slightly from each other, as expected for crystalline samples.

3.6. FTIR spectroscopy

The spectra (4000–1350 cm^{-1}) obtained for α-GeP samples, as well as for α-GeP-100 heat-treated at 300°C and 700°C for 4 h, temperatures at which the anhydrous and the pyrophosphate phases are formed, respectively, are presented in Fig. 7. Since the narrow bands centered at 3547, 3460 and 1622 cm^{-1} decrease proportionally during the dehydration process, and disappear at its end, as demonstrated in the $Ge(HPO_4)_2$ spectrum, we can conclude that these absorption bands are attributed to vibrational modes of interlayer water, the first two referring to the (O–H) stretching modes and the latter to the (H–O–H) deformation mode.

In addition, one can notice, in the same spectrum, the growing in of two intense absorption bands centered at 3223 and 3074 cm^{-1}, which can be attributed to the (O–H) stretching mode of free P–O–H groups. A similar

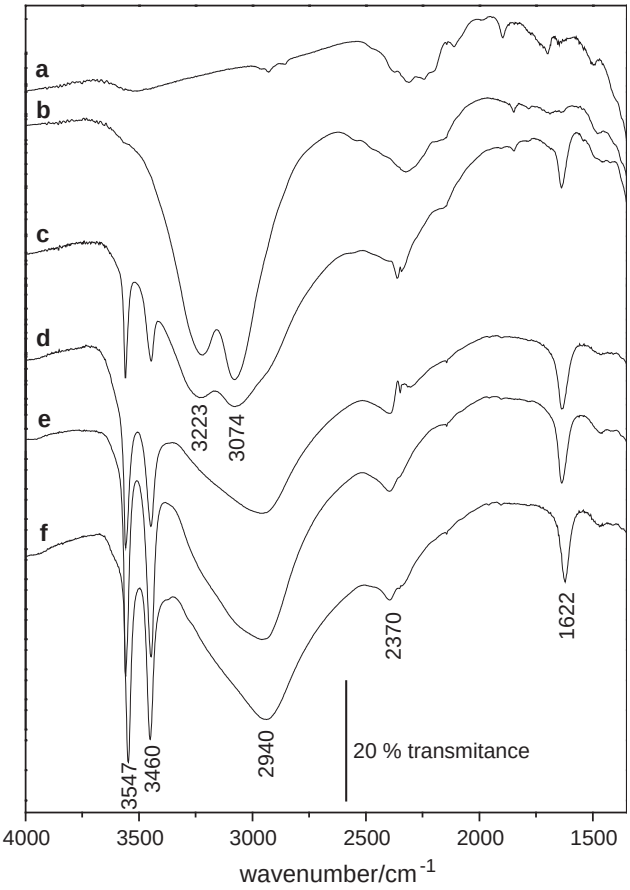

Fig. 7. FTIR spectra (4000–1350 cm^{-1}) for the samples: (a) GeP_2O_7; (b) $Ge(H_2PO_4)_2$; (c) α-GeP-14; (d) α-GeP-25; (e) α-GeP-100; (f) α-GeP-720.

result was obtained by Horsley et al. concerning α-ZrP [32], although a single absorption band centered at 3280 cm^{-1} was observed in this case. A probable reason for the observation of two stretching (O–H) modes in the spectrum of the anhydrous α-GeP comes from the existence of hydrogenphosphate groups showing different (P)O–H distances even after the elimination of interlayer water. Notwithstanding, as one can infer from the ^{31}P MAS NMR spectrum obtained for this sample and shown in Fig. 6c, the observation of two different (P)O–H distances do not lead to detectable discrepancies in the electronic environment of the phosphorus nuclei.

After the heat-treatment at 700°C, absorption bands centered at 3223 and 3074 cm^{-1} were eliminated from the spectrum. Since the phase obtained at this temperature is the pyrophosphate, formed by the elimination of structural water, it corroborates the assignment of these two bands to free P–O–H groups. This process involves condensation of adjacent layers leading to the formation of P–O–P bonds with elimination of water.

The formation of hydrogen bonds increases the intramolecular O–H distance, reducing its oscillation frequency. Thus the band at 2940 cm^{-1}, present in the spectra of α-GeP samples, is assigned to the ((P)O–H)

stretching mode of hydrogen bonded phosphate groups. The asymmetry of this band could be associated to the presence of an absorption band at the region around 3160 cm^{-1}, also attributed to an O–H stretching mode of interlayer water molecules resultant of their loss of symmetry. Although it is not visible in the α-GeP spectra, this band occurs as a well-defined shoulder in the spectra of α-ZrP and α-HfP [32,33].

The spectrum of the pyrophosphate phase shows a set of absorption bands near 2370 cm^{-1}, also observed in the spectra of α-GeP and its anhydrous form $[Ge(HPO_4)_2]$. Since this set of bands was not eliminated in the heat treatments, we can conclude these bands are assigned to overtones of the P–O stretching modes encountered in the region between 1200 and 950 cm^{-1} (Fig. 8).

An examination of the evolution of the bands in the spectra of α-GeP samples clearly characterizes a structural short-range organization of the solid as the steps of preparation were performed. This organization is shown by the intensification and narrowing of the bands at 3547 and 3460 cm^{-1}, attributed to interlayer water stretching modes, suggesting a progressive ordering of water molecules in the lattice, as pointed out by thermogravimetric analysis.

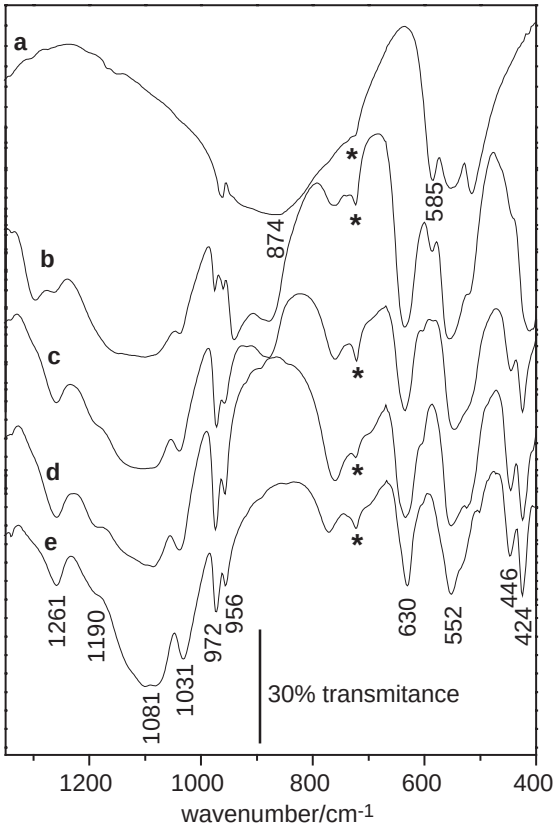

Fig. 8. FTIR spectra (1350–400 cm^{-1}) for the samples: (a) GeO_2; (b) α-GeP-14; (c) α-GeP-25; (d) α-GeP-100; (e) α-GeP-720. *Nujol band.

The spectra obtained for α-GeP samples, as well as for the precursor GeO_2, in the region from 1350 to 400 cm^{-1}, are presented in Fig. 8.

The spectra of α-GeP samples show two sets of absorption bands. The five bands occurring between 1200 and 900 cm^{-1} are assigned to P–O stretching modes and the four between 650 and 400 cm^{-1} are attributed to O–P–O deformation modes [34]. The absorption band at 1261 cm^{-1}, attributed to the P–O–H deformation mode, is the first evidence of short-range structural organization of the solid, since one can observe it becomes more defined after each preparation step. Such behavior is also observed for the bands assigned to stretching and deformation modes of the phosphate groups. These features indicate that the steps adopted in the treatment led to progressively more organized solids.

Besides providing the accompaniment of the short-range structural evolution of the solids, Fig. 8 also permitted us to recognize the real absence of GeO_2 in the composition of the α-GeP-100 and α-GeP-720 samples, confirming the earlier results, since the bands of the oxide centered at 874 and 585 cm^{-1} were observed only for the samples α-GeP-14 and α-GeP-25, which also agrees with the XRD powder results.

3.7. Scanning electron microscopy

Scanning electron microscopic observations (Fig. 9) reveal that every preparation step was followed by a severe morphological evolution of the solid. Firstly, one can notice that the micrograph obtained for sample α-GeP-14 shows a morphology completely unlike the following ones, being characterized basically by big aggregates. Together with results already described, this observation once more shows the biphasic nature of this sample.

From the next sample (α-GeP-25) onward, micrographs show the formation and the evolution of a plate-like morphology, culminating in obtaining planar pseudo-hexagonal crystallites with size distributions from 1 to 5 μm for the sample α-GeP-720. This observation agrees with the results obtained for XRD powder, since diffraction theory prevents the narrowing of the peaks as the average size of the crystallites increases.

4. Conclusions

Pure-phase and high crystalline α-GeP showing the minimal formulae $Ge(HPO_4)_2 \cdot H_2O$ was synthesized in this work. The low chemical stability of α-GeP, which is the probable reason for the reduced number of studies concerning this material and which makes its hydrothermal treatment under severe conditions impossible, was successfully overcame here by using softer

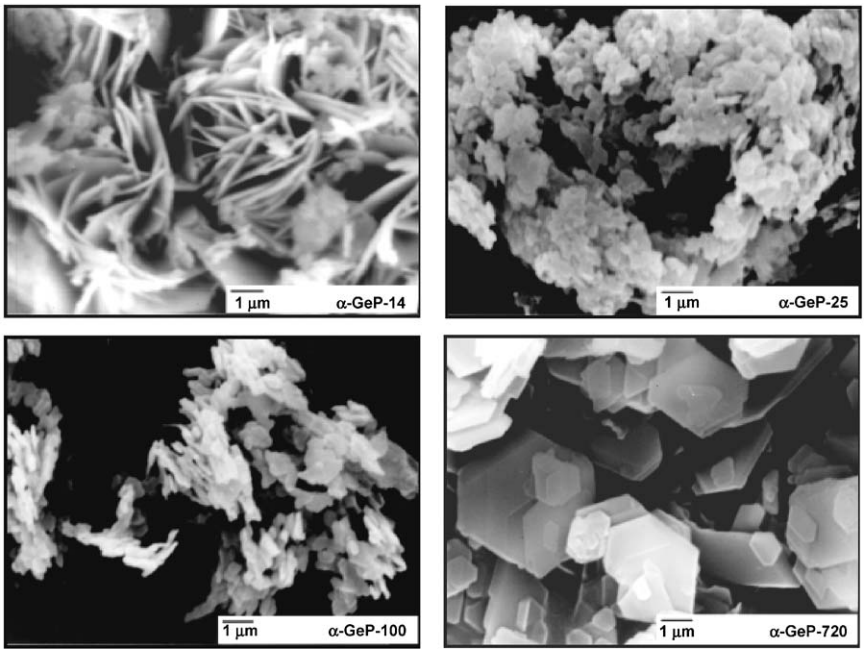

Fig. 9. Scanning electron micrographs of the α-GeP samples.

conditions and extended periods to obtain materials showing increased crystallinity, suitable for the exploration of the intercalation properties of α-GeP, a subject that is, thus far, totally absent in the literature.

Acknowledgments

The authors are grateful to CAPES and PRONEX (Proc. No. 11P22810-97) for the financial support. This is a contribution of Millennium Institute for complex materials.

References

[1] A. Clearfield, J. Stynes, J. Inorg. Nucl. Chem. 26 (1964) 117.
[2] A. Clearfield, G.D. Smith, Inorg. Chem. 8 (1969) 431.
[3] G. Alberti, Acc. Chem. Res. 11 (1978) 163.
[4] M.H. Herzog-Cance, D.J. Jones, R. El-Mejjad, J. Rozière, J. Tomkinson, J. Chem. Soc. Faraday Trans. 88 (1992) 2275.
[5] J.E. Pillion, M.E. Thompson, Chem. Mater. 3 (1991) 777.
[6] D.J. Maia, M.A. De Paoli, O.L. Alves, A.J.G. Zarbin, S. Das Neves, Quim. Nova 23 (2000) 204.
[7] Y. Ding, D.J. Jones, P. Maireles-Torres, J. Rozière, Chem. Mater. 7 (1995) 562.
[8] K.J. Chao, T.C. Chang, S.Y. Ho, J. Mater. Chem. 3 (1993) 427.
[9] G. Cao, T.E. Mallouk, J. Solid State Chem. 94 (1991) 59.
[10] A.B. Gonçalves, A.S. Mangrich, A.J.G. Zarbin, Synth. Metals 114 (2000) 119.
[11] D.J. Maia, O.L. Alves, M.-A. De Paoli, Synth. Metals 90 (1997) 37.
[12] A.J.G. Zarbin, D.J. Maia, M.-A. De Paoli, O.L. Alves, Synth. Metals 102 (1999) 1277.
[13] D.A. Everest, J. Chem. Soc. 4 (1953) 4117.
[14] B. Lelong, Ann. Chim. France 9 (1964) 229.
[15] K.A. Avduevskaya, I.V. Tananaev, Russ. J. Inorg. Chem. 8 (1963) 527.
[16] K.A. Avduevskaya, I.V. Tananaev, Russ. J. Inorg. Chem. 10 (1965) 197.
[17] A. Winkler, E. Thilo, Z. Anorg. Allg. Chem. 346 (1966) 92.
[18] A. La Ginestra, P. Galli, M.L. Berardelli, M.A. Massucci, J. Chem. Soc. Dalton Trans. 4 (1984) 527.
[19] A.N. Christensen, E.K. Andersen, I.G.K. Andersen, G. Alberti, M. Nielsen, M.S. Lehman, Acta Chem. Scand. 44 (1990) 865.
[20] J.M. Troup, A. Clearfield, Inorg. Chem. 16 (1977) 3311.
[21] P. Patrono, A. La Ginestra, C. Ferragina, M.A. Massucci, A. Frezza, S. Vecchio, J. Thermal Anal. 38 (1992) 2603.
[22] H. Hayashi, K. Torii, S. Nakata, J. Mater. Chem. 7 (1997) 557.
[23] P. Galli, A. La Ginestra, M.L. Berardelli, M.A. Massucci, P. Patrono, Thermochim. Acta 92 (1985) 615.
[24] A. La Ginestra, P. Patrono, A. Frezza, C. Mancini, M.A. Massucci, S. Vecchio, J. Thermal Anal. 40 (1993) 1223.
[25] J. Rodríguez-Carvajal, Phys. B 192 (1993) 55.
[26] L.G. Berry, B. Post, S. Weissmann, H.F. McGurdie, W.F. McClune (Eds.), Powder Diffraction File Search Manual—Inorganic, Joint Committee On Powder Diffractions Standards, Pennsylvania, 1973.
[27] U. Costantino, A. La Ginestra, Thermochim. Acta 52 (1982) 179.
[28] J. Albertsson, A. Oskarsson, R. Tellgren, J.O. Thomas, J. Phys. Chem. 81 (1977) 1574.
[29] N.J. Clayden, J. Chem. Soc. Dattton Trans. 8 (1987) 1877.
[30] D.J. Maclachlan, K.R. Morgan, J. Phys. Chem. 94 (1990) 7656.
[31] H. Nakayama, T. Eguchi, N. Nakamura, S. Yamagushi, M. Daniyo, M. Tsuako, J. Mater. Chem. 7 (1997) 1063.
[32] S.E. Horsley, D.V. Nowell, D.T. Stewart, Spectrochim. Acta A 30 (1974) 535.
[33] R.B. Dushin, V.N. Krylov, K.P. Larina, B.P. Nikolskii, Bull Acad. Sci. USSR 3 (1977) 469.
[34] D.E.C. Corbridge, in: M. Grayson, E.J. Griffith (Eds.), Topics in Phosphorous Chemistry, Wiley, New York, 1970, p. 241.